Interaction of solitons in one-dimensional dipolar Bose-Einstein condensates and formation of soliton molecules

B. B. Baizakov,[1,*] S. M. Al-Marzoug,[2,3] and H. Bahlouli[2,3]
[1]*Physical-Technical Institute, Uzbek Academy of Sciences, 100084 Tashkent, Uzbekistan*
[2]*Physics Department, King Fahd University of Petroleum and Minerals, Dhahran 31261, Saudi Arabia*
[3]*Saudi Center for Theoretical Physics, Dhahran 31261, Saudi Arabia*
(Received 3 February 2015; published 8 September 2015)

The interaction between two bright solitons in a one-dimensional dipolar Bose-Einstein condensate (BEC) is investigated, with the aim of finding the regimes where they form a stable bound state, known as the soliton molecule. To study soliton interactions in BECs we employed a method similar to that used in experimental investigation of the interaction between solitons in optical fibers. The idea consists in creating two solitons at some spatial separation from each other at initial time t_0 and then measuring the distance between them at a later time $t_1 > t_0$. Depending on whether the distance between solitons has increased, decreased, or remained unchanged, compared to its initial value at t_0, we conclude that the soliton interaction was repulsive, attractive, or neutral, respectively. We propose an experimentally viable method for estimating the binding energy of a soliton molecule, based on its dissociation at critical soliton velocity. Our theoretical analysis is based on the variational approach, which appears to be quite accurate in describing the properties of soliton molecules in dipolar BECs, as reflected in the good agreement between the analytical and the numerical results.

DOI: 10.1103/PhysRevA.92.033605 PACS number(s): 67.85.Hj, 03.75.Kk, 03.75.Lm

I. INTRODUCTION

The interaction of solitons has been a subject of great interest right from the beginning of the early investigations [1]. New fundamental features of soliton interactions are still being discovered; the existence of a phase-dependent spatial jump in the trajectories of two colliding matter-wave solitons, reported in a recent experiment [2], is just one example. Apart from their scientific importance, soliton interactions have a practical importance. For instance, interaction between optical solitons sets the limit on the rate of information transfer in fiber-optic communication systems [3]. Due to their important applications, soliton interactions have been extensively studied, both theoretically and experimentally, in optical fibers [4–7], photonic crystals [8], and plasmas [9]. Recent experimental studies have shown that, in addition to interactions between neighboring optical solitons in close proximity, there exists a long-range interaction between them [10]. The generation of spatially separated coherent matter-wave packets and their subsequent interaction constitute the basic phenomena in the operation of modern atomic interferometers [11] working in the solitonic regime [12,13] where the fringe visibility is significantly increased compared with an ordinary atomic cloud, as demonstrated in [12].

Solitons have been experimentally observed in many areas of physics, including Bose-Einstein condensates (BECs) [14–16]. Experiments with solitons in BECs reported so far have been concerned with the creation of solitons and study of their collective dynamics. Regarding the type of interaction between matter-wave solitons a conjecture was made based on the behavior of neighboring solitons in a soliton train [17]. Meanwhile, it would be interesting to explore systematically the interaction between two matter-wave solitons with varying spatial separations and relative phases. Recent progress in controlled creation and manipulation of matter-wave solitons in BECs [2,15,16] indicates that such experiments on soliton interactions are now within the scope of the current technology. A key role belongs to a minimally destructive polarization phase-contrast imaging technique [18], which allows one to make multiple imaes of the soliton pair during a single experimental run, as reported recently with regard to phase-dependent collision of two matter-wave solitons [2]. An essentially new method reported in Ref. [16] for controlled (i.e., deterministic in both soliton position and momentum) creation of matter-wave bright solitons and soliton pairs without the use of Feshbach resonances opens new perspectives for the investigation of soliton interactions in BECs with unprecedented accuracy.

Experimental realization of chromium BECs with long range dipole-dipole atomic interactions [19] has opened a new direction in the physics of ultracold quantum gases. Subsequently two other species with strong dipolar interactions, namely, dysprosium [20] and erbium [21], were Bose-condensed. The principal difference of chromium condensates from alkali-metal atom condensates is that ^{52}Cr has the large permanent magnetic dipole moment $d = 6\,\mu_B$, where $\mu_B = e\hbar/2m_e$ is the Bohr magneton. Since the dipole-dipole force is proportional to the square of the magnetic moment, the dipolar interaction in chromium condensates is a factor of 36 times stronger than in alkali-metal atom condensates, like ^{87}Rb ($d = 1\,\mu_B$). Similar arguments pertain also for other dipolar quantum gases, ^{164}Dy ($d = 10\,\mu_B$) and ^{168}Er ($d = 7\,\mu_B$).

In this work we study, by means of variational approximation (VA) and numerical simulations, the interaction between two bright solitons in a one-dimensional (1D) dipolar BEC. We employ a strategy similar to that used in the experimental investigation of interaction forces between fiber-optic solitons [5,22]. Following that idea in numerical experiments we create two bright solitons at some initial spatial separation, then give the pair a chance to evolve for some period of time, and,

*baizakov@uzsci.net

finally, measure the distance between the solitons when the evolution time has elapsed. Depending on whether the distance between the solitons has increased, decreased, or remained unchanged, compared to its initial value, we conclude that the type of soliton interaction is repulsive, attractive, or neutral, respectively.

There is a qualitative difference between solitons in dipolar and those in nondipolar media. Specifically, two antiphase solitons in a dipolar medium attract each other at a large separation and repel at a short separation. Due to this property they can form stable bound states with nonzero binding energy, whereas in nondipolar media they always repel and never form a stable bound state. The possibility of a molecular type of interaction between solitons in a dipolar BEC moving in two neighboring waveguides was shown in [23]. The existence of stable multisoliton structures in a 2D dipolar BEC was also reported in [24].

Our main objective in this work is to find the conditions under which two interacting solitons in the same quasi-1D waveguide form a stable bound state, which can be considered a basic matter-wave soliton molecule. When a stable bound state of two solitons has been realized, we characterize the soliton molecule by its bond length and binding energy. Our work distinguishes itself from other relevant publications in that we use the VA with a Gauss-Hermite ansatz and analytically tractable function of nonlocality (response function), which allows us to describe the essential features of soliton molecules in a dipolar BEC. Moreover, we provide a detailed comparison of predictions of VA with the results of numerical simulations of the Gross-Pitaevskii equation (GPE).

The paper is organized as follows. In the next section (Sec. II) we introduce the governing equation and develop the VA for the dynamics of soliton molecules in a dipolar BEC. In Sec. III we use an optimization procedure to find the shape of a soliton molecule and validate the VA by comparing the analytical predictions with the results of numerical simulations. In Sec. IV we present such important characteristics of a soliton molecule as its binding energy. In Sec. V we reveal the character of soliton interactions in a dipolar BEC using a method borrowed from the field of fiber-optic solitons. In Sec. VI we summarize our findings.

II. THE GOVERNING EQUATION AND VARIATIONAL APPROACH

From the viewpoint of theoretical description, matter-wave solitons in BECs and optical solitons in fibers are similar. The mean-field GPE for the dynamics of BECs and the nonlinear Schrödinger equation for propagation of optical solitons in fibers have a formal analogy. The similarity of the basic equations has been fruitful in transferring many ideas from nonlinear optics to the field of matter waves [25]. In this paper we transfer one more idea, concerning soliton interactions, from the field of fiber optics into the field of BECs.

We consider the 1D GPE by taking into account both local and nonlocal nonlinearities, which account for the usual contact interactions between atoms, and long-range dipole-dipole interactions [26,27],

$$i\frac{\partial\psi}{\partial t}+\frac{1}{2}\frac{\partial^2\psi}{\partial x^2}+q|\psi|^2\psi + g\psi\int_{-\infty}^{+\infty}R(|x-\xi|)\,|\psi(\xi,t)|^2d\xi=0, \tag{1}$$

where $q=a_s/|a_{s0}|$ is the coefficient of contact interactions, controlled by the atomic s-wave scattering length a_s, with a_{s0} being its background value; $g=a_d/|a_{s0}|$ is the coefficient of nonlinearity, responsible for the long-range dipolar atomic interactions, expressed via the characteristic dipole length $a_d=\mu_0 d^2 m/(12\pi\hbar^2)$, with m and d being the mass and magnetic dipole moment of atoms, respectively, oriented along the x axis; and μ_0 is the permeability of the vacuum. Time and space are expressed in units of $t_0=\omega_\perp^{-1}$ and $l_0=\sqrt{\hbar/(m\omega_\perp)}$, respectively, with $\omega_\perp$ being the frequency of radial confinement. The wave function is re-scaled as $\psi=\sqrt{2|a_{s0}|}\Psi$ and normalized to the reduced number of atoms in the condensate $N=\int_{-\infty}^{+\infty}|\psi(x)|^2dx$, which is a conserved quantity of Eq. (1). The following two models for the kernel (nonlocal response functions) are relevant to dipolar condensates confined to quasi-1D traps:

$$R_1(x)=(1+2x^2)\,\exp(x^2)\,\mathrm{erfc}(|x|)-2\pi^{-1/2}|x|, \tag{2}$$

$$R_2(x)=\delta^3(x^2+\delta^2)^{-3/2}. \tag{3}$$

The former kernel was derived for the dipolar BEC using the single-mode approximation [28], while the latter, containing a cutoff parameter, δ, was proposed in Ref. [26] and is more convenient for analytical treatment. Making use of the matching conditions

$$R_1(0)=R_2(0)\quad\text{and}\quad\int_{-\infty}^{\infty}R_1(x)dx=\int_{-\infty}^{\infty}R_2(x)dx, \tag{4}$$

which requires $\delta=\pi^{-1/2}$, one can take advantage of the simplicity of $R_2(x)$ for the application of VA. The meaning of δ is the effective size of the dipole. Actually, it takes the value of the order of the transverse confinement length, which makes the model 1D, and sets the unit length in Eq. (1). Therefore, the choice of $\delta=\pi^{-1/2}\approx 0.56$ is quite reasonable. In the limit $x\gg\delta$, where dipole-dipole interaction effects dominate the contact interaction effects, both response functions behave as $\sim 1/x^3$. This justifies the application of the kernel function $R_2(x)$ for analytical treatment of dipolar effects in a BEC. By comparing the graphics of these two response functions one can be convinced that indeed $R_1(x)$ and $R_2(x)$ match very closely [26].

The Lagrangian density generating Eq. (1) is

$$\mathcal{L}=\frac{i}{2}(\psi\psi_t^*-\psi^*\psi_t)+\frac{1}{2}|\psi_x|^2-\frac{q}{2}|\psi|^4-\frac{g}{2}|\psi(x,t)|^2 \times\int_{-\infty}^{\infty}R(x-\xi)|\psi(\xi,t)|^2d\xi. \tag{5}$$

To study soliton interactions in a dipolar BEC we need to develop the VA for a two-soliton molecule. To this end we employ a Gauss-Hermite trial function, which was successful in the description of soliton molecules in dispersion-managed

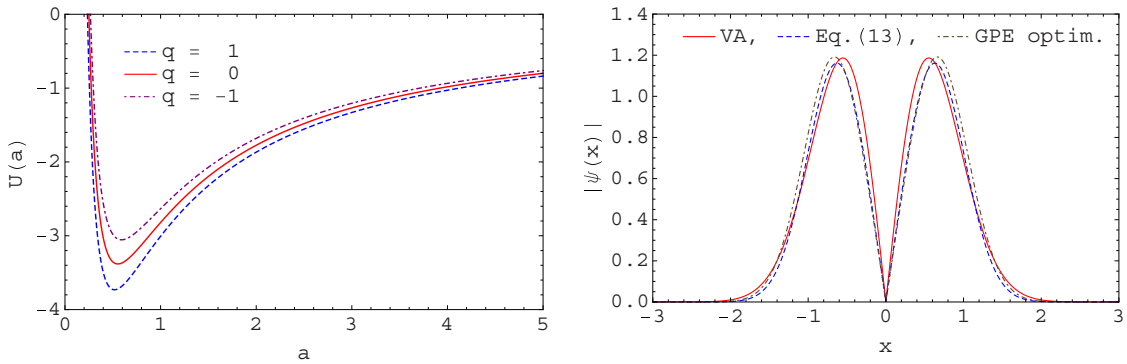

FIG. 1. (Color online) Left: A molecular-type potential associated with VA, Eq. (10), for different strengths of the contact interaction. Right: The shape of a two-soliton molecule in a pure dipolar BEC with $N = 2$, $q = 0$, $g = 20$ as predicted by VA with the trial function, (6), for $A = 3.538$, $a = 0.553$, $N = 1.876$ [solid (red) line], predicted by two antiphase Gaussian functions with parameters given in Eq. (7) [dashed (blue) line], and found from the numerical optimization procedure, applied to the GPE, (1) [dash-dotted (brown) line]. The minimum of the effective potential $U(a)$ is attained at $a_0 = 0.53$, and the equilibrium distance between center-of-mass positions of pulses predicted by Eq. (7) is $\Delta_0 = 4a_0/\sqrt{\pi} \simeq 1.2$, while the GPE optimization gives $\Delta_0 \simeq 1.3$.

optical fibers [29],

$$\psi(x,t) = A(t)\,x\,\exp\left[-\frac{x^2}{2a(t)^2} + ib(t)x^2 + i\phi(t)\right], \quad (6)$$

where $A(t)$, $a(t)$, $b(t)$, and $\phi(t)$ are variational parameters, associated with the amplitude, width, chirp, and phase, respectively. The norm $N = \int |\psi(x)|^2 dx = A^2 a^3 \sqrt{\pi}/2$ is proportional to the number of atoms in the condensate. For specified values of A and a, the waveform, (6), can be well approximated by two antiphase Gaussian functions with amplitude A_0, width a_0, and half-separation x_0:

$$A_0 = \frac{2Aa}{\sqrt{\pi}} e^{-2/\pi}, \quad a_0 = \frac{\pi a}{16} e^{4/\pi}, \quad x_0 = \frac{2a}{\sqrt{\pi}}. \quad (7)$$

Substitution of the ansatz, (6), and response function, (3), into the Lagrangian density, (5), and subsequent integration over the space variable x yield the averaged Lagrangian,

$$\frac{L}{N} = \frac{3}{2}a^2 b_t + \phi_t + \frac{3}{4a^2} + 3a^2 b^2 - \frac{3\,q\,N}{8\sqrt{2\pi}\,a} - \frac{3\,g\,\delta\,N}{8\sqrt{2}\,a} \times \left[\mathcal{U}\left(\frac{1}{2},0,z\right) - \frac{\delta^2}{3a^2}\mathcal{U}\left(\frac{3}{2},1,z\right) + \frac{\delta^4}{4a^4}\mathcal{U}\left(\frac{5}{2},2,z\right)\right], \quad (8)$$

where

$$\mathcal{U}(\mathrm{a},\mathrm{b},z) = \frac{1}{\Gamma(\mathrm{a})}\int_0^\infty e^{-zt} t^{\mathrm{a}-1}(t+1)^{\mathrm{b}-\mathrm{a}-1} dt \quad (9)$$

is the confluent hypergeometric function [30], and $z = \delta^2/(2a^2)$.

The VA equation for the parameter a of the two-soliton molecule, which is proportional to the separation between solitons, can be derived from the Euler-Lagrange equations $d/dt(\partial L/\partial \nu_t) - \partial L/\partial \nu = 0$ for variational parameters $\nu \to a, b, \phi$, using the averaged Lagrangian, (8):

$$a_{tt} = \frac{1}{a^3} - \frac{q\,N}{4\sqrt{2\pi}\,a^2} - \frac{g\delta\,N}{4\sqrt{2}a^2}\left[\mathcal{U}\left(\frac{1}{2},0,z\right) - 3z\mathcal{U}\left(\frac{3}{2},1,z\right) + 7z^2\mathcal{U}\left(\frac{5}{2},2,z\right) - 5z^3\mathcal{U}\left(\frac{7}{2},3,z\right)\right]. \quad (10)$$

The corresponding effective potential $U(a)$ for the width is depicted in Fig. 1 (left). The analytic form of the potential $U(a)$, which can be found by integrating the right-hand side of Eq. (10), is rather complicated and we do not show it here explicitly. The fixed point $a_{tt} = -\partial U(a)/\partial a = 0$ of this equation, a_0, is associated with the stationary separation between center-of-mass positions of two solitons constituting the molecule $\Delta_0 = 2x_0 = 4a_0/\sqrt{\pi}$. At a larger separation ($a > a_0$) the solitons attract each other ($\partial U/\partial a > 0$), and at a smaller separation ($a < a_0$) they repel ($\partial U/\partial a < 0$), therefore the effective potential $U(a)$ has a property of the molecular type. Figure 1 (right) illustrates the shape of a two-soliton molecule, as predicted by VA, by two antiphase Gaussian functions with parameters given in Eq. (7), and by the optimization procedure, applied to the GPE, (1), described in the next subsection.

When solitons of the molecule are placed in their equilibrium positions, they stay motionless, as shown in Fig. 2. If solitons are slightly displaced and released, they perform low-amplitude oscillations around their stationary separation. The dynamics of the molecule strongly depends on the initial phase difference between solitons. In particular, even a slight deviation from the antiphase configuration leads to periodic exchange of atoms between solitons. At larger deviations the soliton molecule does not form.

The frequency of soliton oscillations near the equilibrium state can be estimated from a linearized version of Eq. (10):

$$\Omega_0^2 = \frac{3}{a_0^4} - \frac{Nq}{2\sqrt{2\pi}\,a_0^3}\frac{\delta g N}{4\sqrt{2}a_0^3} \times \left[-15z_0^2\mathcal{U}\left(\frac{5}{2},0,z_0\right) + 21z_0^2\mathcal{U}\left(\frac{5}{2},1,z_0\right) - 9z_0^2\mathcal{U}\left(\frac{5}{2},2,z_0\right) + 20z_0\mathcal{U}\left(\frac{3}{2},-1,z_0\right) - 28z_0\mathcal{U}\left(\frac{3}{2},0,z_0\right) + 13z_0\mathcal{U}\left(\frac{3}{2},1,z_0\right) - 2\mathcal{U}\left(\frac{1}{2},0,z_0\right)\right]. \quad (11)$$

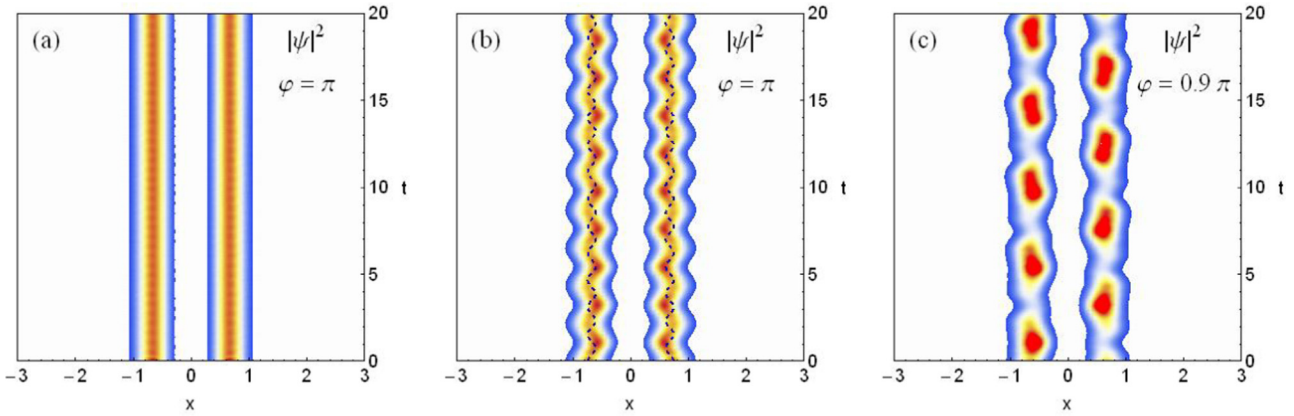

FIG. 2. (Color online) (a) Stable propagation of a two-soliton molecule composed of two antiphase ($\varphi = \pi$) Gaussian pulses with parameters $A_0 = 1.196$, $a_0 = 0.394$, placed at their equilibrium positions $x_0 = \pm 0.657$. (b) When the solitons are slightly displaced (by 20%) from equilibrium positions, they perform oscillations. The density plot $|\psi|^2$ is obtained by numerical solution of the GPE, (1). The dashed line corresponds to calculations according to the VA equation, (10), which shows increasing phase shift with respect to GPE. (c) Periodic exchange of atoms between two solitons when the initial phase difference is slightly decreased.

For the period of oscillations near the stationary separation we have $T_{\rm VA} = 2\pi/\Omega_0 \simeq 1.54$. The prediction of VA is in qualitative agreement with the result of numerical simulation of the GPE, $T_{\rm GPE} \simeq 2.2$ (see Fig. 2). In general, the VA provides a fairly good description of the static and dynamic properties of the soliton molecule, while its waveform remains close to the selected trial function, (6). The agreement between VA and GPE deteriorates at large separations between solitons, close to the dissociation point, where the trial function cannot be well approximated by two antiphase Gaussian functions.

III. IMPROVING THE SHAPE OF THE SOLITON MOLECULE BY THE OPTIMIZATION PROCEDURE

The VA provides the approximate waveform of a soliton molecule. When a trial function with parameters, defined by the stationary solution of VA equation, is assigned as the initial condition for the GPE, low-amplitude oscillations of the molecule's shape and separation between pulses are observed. This implies that the soliton molecule is in its excited state.

For some precise parameter calculations, such as the binding energy of soliton molecules, a true ground state should be employed. In Ref. [31] an optimization strategy to find the stationary shape of a soliton molecule in dispersion-managed optical fibers was proposed. Below we extend this approach to soliton molecules in a dipolar BEC. It is based on the Nelder-Mead nonlinear optimization procedure [32], which seeks to minimize an objective (or cost) function

$$f = \frac{1}{N_0}\int_{-\infty}^{\infty}(|\psi(x,0)| - |\psi(x,t_1)|)^2\,dx, \qquad N_0 = \int_{-\infty}^{\infty}|\psi(x,0)|^2\,dx, \tag{12}$$

where

$$\psi(x,0) = A_0\left(\exp\left[-\frac{(x-x_0)^2}{2a_0^2}\right] - \exp\left[-\frac{(x+x_0)^2}{2a_0^2}\right]\right) \tag{13}$$

is the initial waveform, composed of two antiphase Gaussian functions, separated by a distance $2x_0$, and $\psi(x,t_1)$ is the result of evolution of $\psi(x,0)$ for some period of time $t = t_1$, according to the GPE. The normalization factor N_0 in Eq. (12) is introduced to avoid trivial solutions, in particular, corresponding to $x_0 = 0$. In the general case minimization of the objective function can be performed with respect to variables a_0 and x_0, since the amplitude A_0 is fixed by the norm of the Gaussian. However, numerical experiments show that VA-predicted values of a_0 and A_0 for a single soliton are quite accurate, and minimization only with respect to pulse separation x_0 can produce the stationary state of the molecule. The evolution time t_1 can be estimated as a half-period of oscillation for the molecule $t_1 = \pi/\Omega_0$. Although the Nelder-Mead optimization procedure finds the minimum of the objective function, (12), for Gaussian functions with a broad range of parameters, the convergence rate can be improved by selecting the initial waveform close to the stationary state. The VA can provide a waveform which is close to the stationary state. We find the stationary pulse separation x_0 and norm of the soliton molecule N from the Nelder-Mead optimization procedure. The obtained results were confirmed by an alternative method of Luus-Jaakola [33,34]. Our preference for these optimization methods is motivated by several of their advantages, such as the simplicity of programming (since calculation of function derivatives is not required), high convergence rate, and reliability and effectiveness of locating the global minimum of the objective function.

IV. INTERACTION POTENTIAL AND BINDING ENERGY OF SOLITON MOLECULES

The binding energy of a soliton molecule E_b can be defined as the amount of energy which is required for dissociation of the molecule into two separate individual free solitons, far away from each other. In numerical simulations using the GPE, the process of dissociation can be implemented by assigning an initial velocity to each soliton in opposite directions,

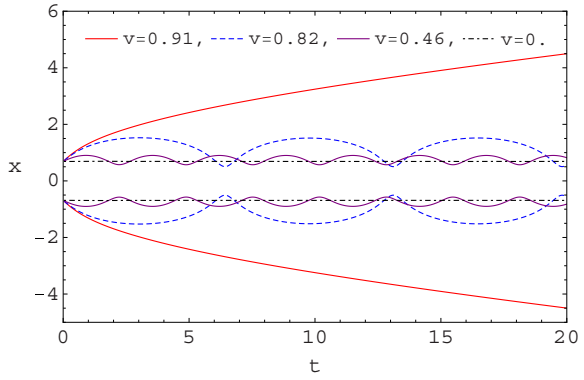

FIG. 3. (Color online) Dynamics of the centers of masses of two solitons, forming the molecule, when the two solitons are set in motion at different velocities in opposite directions. When the velocity is less than critical $v < v_{cr} = 0.91$, solitons perform oscillations near equilibrium positions. At critical velocity the molecule dissociates into freely moving individual solitons [solid (red) lines].

$\psi = \psi_1 e^{ivx} + \psi_2 e^{-ivx}$. If the velocity is lower than some critical value $v < v_{cr}$, solitons perform oscillations around their stationary positions; otherwise the molecule disintegrates into individual solitons, traveling in opposite directions, as illustrated in Fig. 3.

In a "particle in potential well" picture this situation corresponds to the escape of the particle from the potential well at the critical kinetic energy. The critical velocity determines the binding energy of the molecule $E_b \sim v_{cr}^2/2$. Figure 4 illustrates the potential of interactions between the two solitons, normalized to the binding energy, as a function of the distance between solitons in units of stationary separation x_0. To construct the potential $U(x)$ we assign a velocity to solitons and determine the maximal and minimal values of the separation, which correspond to right and left classical turning points of the oscillating particle in the potential well. Repeating these calculations for velocities in the range $v \in [0, v_{cr}]$ we construct the potential, shown at the left in Fig. 4. As expected, the bigger norm N (or number of atoms) of the molecule corresponds to stronger potential, connecting solitons.

The critical velocity v_{cr}, at which the molecule disintegrates into far-separated individual solitons, is determined from GPE simulations by setting the two bound solitons into motion in opposite directions, as shown in Fig. 4. In the experiment, pushing the solitons in opposite directions can be realized by means of a laser beam, directed into the center of the molecule, as used to split the condensate in two halves [2]. The intensity of the laser beam can be varied to give the desired initial velocity to solitons.

About the repulsive interaction between two antiphase solitons the following comment is appropriate. As experimentally demonstrated in [2] and theoretically shown in [35], two colliding wave packets exchange not only velocities (as classical particles do), but also their entire wave functions (as quantum mechanical particles do via the tunnel phenomenon). In our case of equal masses of two colliding solitons, the classical and quantum descriptions lead to the same result. Physically, the repulsive interaction of antiphase matter-wave solitons can be regarded as the exchange of velocities of two colliding classical particles interacting via a hard-core potential.

V. NUMERICAL SIMULATION OF TWO-SOLITON INTERACTIONS

In order to study the character of interaction between two matter-wave solitons in numerical experiments we employ an idea similar to that used for optical solitons in fibers [5]. Initially at $t = 0$, two solitons, either in-phase $\phi = 0$ or out-of-phase $\phi = \pi$, are created at some distance Δ_0 from each other. At a later time $t = t_1 > 0$ the distance between solitons is measured again. If the solitons did not interact, the distance between them should not change with respect to its initial value $\Delta_1 = \Delta_0$. If the interaction was attractive, the final measured distance should be less than the initial distance $\Delta_1 < \Delta_0$. Finally, if the interaction was repulsive, the final distance should be greater than the initial distance $\Delta_1 > \Delta_0$. The numerical experiment consists in repeating the above procedure for different values of the initial distance Δ_0, starting from a sufficiently large separation, greatly exceeding the width of the soliton, then reaching short distances where solitons start to overlap.

The result is presented at the left in Fig. 5 as a plot of Δ_1 (final separation) vs Δ_0 (initial separation). When the solitons, comprising the molecule, are out-of-phase ($\phi = \pi$) we see that

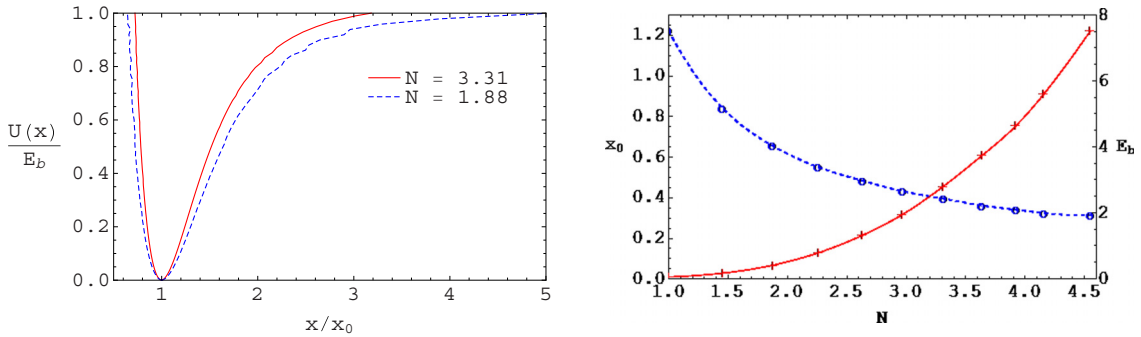

FIG. 4. (Color online) Left: The potential of interaction between two solitons, retrieved from numerical GPE simulation, for two values of the molecule's norm. Similarity to the VA-predicted potential $U(a)$ in Fig. 1 is evident. Right: The stationary half-separation between solitons of the molecule x_0 [dashed (blue) line] and its binding energy E_b [solid (red) line] as a function of the molecule's norm N. Symbols correspond to values found from numerical simulations of the GPE, (1), and lines are interpolating curves for visual convenience.

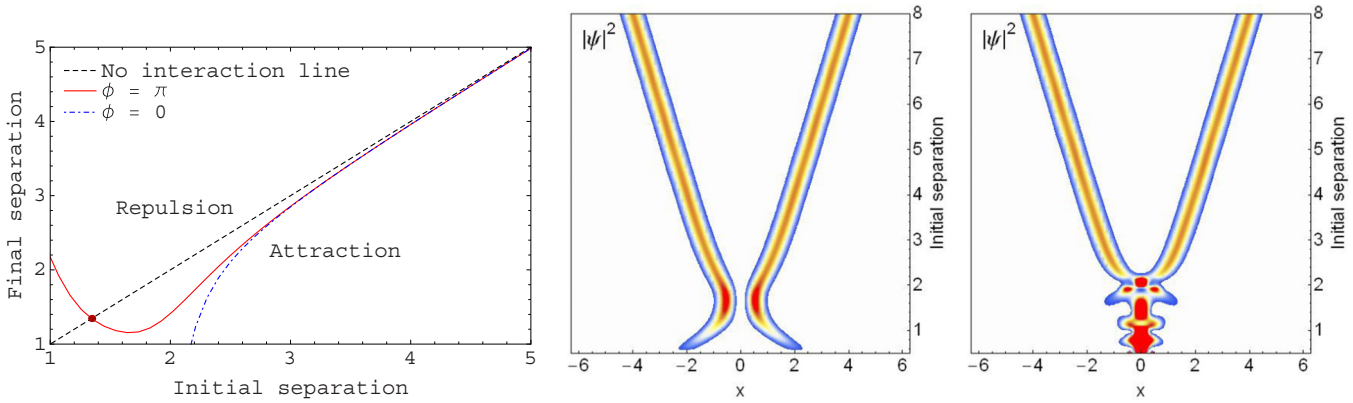

FIG. 5. (Color online) Left: The character of soliton interactions for antiphase and inphase solitons. Antiphase solitons attract each other at large separations and repel at small separations [solid (red) line]. There exists a stationary separation, shown by the filled (red) circle, where attraction changes to repulsion. In-phase solitons always attract and collide [dashed (blue) line]. Middle: The initial separation between two solitons is varied (vertical axis) and the density profiles $|\psi|^2$ at the final time ($t = t_1$) are measured as a function of x. Two antiphase solitons can form a stable soliton molecule at the appropriate initial separation $\Delta_0 \simeq 1.3$. Right: Similar to the middle panel, but for in-phase solitons. Two in-phase solitons always collide and do not form a stable bound state.

at large separations the solitons do not interact [$\Delta_1 \approx \Delta_0$; solid (red) curve is close to the median], while at shorter distances they attract each other [$\Delta_1 < \Delta_0$; solid (red) curve is below the median) until they reach a stationary separation, where again $\Delta_1 = \Delta_0$ [filled (red) circle on the median, where attraction and repulsion are in balance). When solitons are placed at even shorter distances, they repel [$\Delta_1 > \Delta_0$; solid (red) curve is above the median]. That is, the two-soliton molecule behaves like a diatomic molecule. For in-phase solitons ($\phi = 0$) we see that solitons attract each other until their separation becomes comparable to the width of the soliton, then merge, forming a wave packet, whose shape strongly oscillates. The density profiles associated with solid (red) and dashed (blue) curves are presented in the middle and right panels in Fig. 5, respectively.

The numerical simulations are performed using realistic values of atom numbers and interaction parameters in ^{164}Dy for which $m = 2.7 \times 10^{-25}$ kg, $d = 10\ \mu_B = 9.27 \times 10^{-23}$ A m^2, $a_d = \mu_0 d^2 m/(12\pi\hbar^2) \simeq 7 \times 10^{-9}$ m. The frequency of radial confinement, $\omega_\perp = 2\pi \times 62$ Hz, provides the radial oscillator length $l_0 \simeq 1\ \mu$m and unit of time $t_0 = 2.6$ ms. For parameter values $g_0 = 20$ and $N = 2$ used in numerical simulations we obtain the number of atoms in a two-soliton molecule, $\mathcal{N} = g_0 N l_0/(2a_d) \simeq 3000$. The total number of atoms in the ^{164}Dy condensate was $\mathcal{N} = 15\,000$ [20].

VI. CONCLUSIONS

We have studied the interaction between two bright solitons in a dipolar BEC and found the conditions under which they form a stable bound state. It was revealed, by numerical simulations of the governing nonlocal GPE and corresponding variational analysis, that two antiphase solitons in dipolar condensates behave similarly to a diatomic molecule. Namely, they attract each other at large separations and repel each other at small separations. There exists a particular distance at which the two solitons remain motionless in their stationary state. Solitons in a weakly perturbed molecule perform low-amplitude oscillations near the equilibrium position, the frequency of which is predicted quite accurately by the developed model. Two in-phase solitons, when placed close to each other, always collide and do not form the bound state. The obtained results can be useful in further studies of the properties of multisoliton bound states in dipolar BECs.

ACKNOWLEDGMENTS

B.B.B. thanks the Department of Physics at King Fahd University of Petroleum and Minerals (KFUPM) and the Saudi Center for Theoretical Physics for the hospitality during his visit. This work was supported by KFUPM under research group Projects No. RG1333-1 and No. RG1333-2.

[1] N. J. Zabusky and M. D. Kruskal, Phys. Rev. Lett. **15**, 240 (1965).
[2] J. H. V. Nguyen, P. Dyke, De Luo, B. A. Malomed, and R. G. Hulet, Nature Phys. **10**, 918 (2014).
[3] A. Hasegawa and Y. Kodama, *Solitons in Optical Communications* (Clarendon Press, Oxford, UK, 1995).
[4] J. P. Gordon, Opt. Lett. **8**, 596 (1983).
[5] F. Mitschke and L. Mollenauer, Opt. Lett. **12**, 355 (1987).
[6] Y. Kodama and K. Nozaki, Opt. Lett. **12**, 1038 (1987); K. Smith and L. F. Mollenauer, *ibid.* **14**, 1284 (1989).
[7] L. F. Mollenauer and J. P. Gordon, *Solitons in Optical Fibers: Fundamentals and Applications* (Academic Press, San Diego, CA, 2006).
[8] G. I. Stegeman and M. Segev, Science **286**, 1518 (1999).
[9] K. E. Lonngren, Plasma Phys. **25**, 943 (1983).
[10] C. Rotschild, B. Alfassi, O. Cohen, and M. Segev, Nature Phys. **2**, 769 (2006); J. K. Jang, M. Erkintalo, S. G. Murdoch, and S. Coen, Nature Photon. **7**, 657 (2013).
[11] A. D. Cronin, J. Schmiedmayer, and D. E. Pritchard, Rev. Mod. Phys. **81**, 1051 (2009); T. Berrada, S. van Frank, R. Bücker,

T. Schumm, J.-F. Schaff, and J. Schmiedmayer, Nature Commun. **4**, 2077 (2013).

[12] G. D. McDonald, C. C. N. Kuhn, K. S. Hardman, S. Bennetts, P. J. Everitt, P. A. Altin, J. E. Debs, J. D. Close, and N. P. Robins, Phys. Rev. Lett. **113**, 013002 (2014).

[13] J. Cuevas, P. G. Kevrekidis, B. A. Malomed, P. Dyke, and R. G. Hulet, New J. Phys. **15**, 063006 (2013); J. Polo and V. Ahufinger, Phys. Rev. A **88**, 053628 (2013); H. Michinel, A. Paredes, M. M. Valado, and D. Feijoo, *ibid.* **86**, 013620 (2012).

[14] S. Burger *et al.*, Phys. Rev. Lett. **83**, 5198 (1999); J. Denschlag *et al.*, Science **287**, 97 (2000); K. E. Strecker *et al.*, Nature **417**, 150 (2002); L. Khaykovich *et al.*, Science **296**, 1290 (2002); S. L. Cornish *et al.*, Phys. Rev. Lett. **96**, 170401 (2006); C. Becker *et al.*, Nat. Phys. **4**, 496 (2008); C. Hamner *et al.*, Phys. Rev. Lett. **106**, 065302 (2011).

[15] A. L. Marchant, T. P. Billam, T. P. Wiles, M. M. H. Yu, S. A. Gardiner, and S. L. Cornish, Nat. Commun. **4**, 1865 (2013).

[16] P. Medley, M. A. Minar, N. C. Cizek, D. Berryrieser, and M. A. Kasevich, Phys. Rev. Lett. **112**, 060401 (2014).

[17] U. Al Khawaja, H. T. C. Stoof, R. G. Hulet, K. E. Strecker, and G. B. Partridge, Phys. Rev. Lett. **89**, 200404 (2002).

[18] C. C. Bradley, C. A. Sackett, and R. G. Hulet, Phys. Rev. Lett. **78**, 985 (1997).

[19] A. Griesmaier, J. Werner, S. Hensler, J. Stuhler, and T. Pfau, Phys. Rev. Lett. **94**, 160401 (2005).

[20] M. Lu, N. Q. Burdick, S. H. Youn, and B. L. Lev, Phys. Rev. Lett. **107**, 190401 (2011); M. Lu, N. Q. Burdick, and B. L. Lev, *ibid.* **108**, 215301 (2012); Y. Tang, N. Q. Burdick, K. Baumann, and B. L. Lev, New J. Phys. **17**, 045006 (2015).

[21] K. Aikawa, A. Frisch, M. Mark, S. Baier, A. Rietzler, R. Grimm, and F. Ferlaino, Phys. Rev. Lett. **108**, 210401 (2012); K. Aikawa, A. Frisch, M. Mark, S. Baier, R. Grimm, and F. Ferlaino, *ibid.* **112**, 010404 (2014).

[22] M. Stratmann, T. Pagel, and F. Mitschke, Phys. Rev. Lett. **95**, 143902 (2005); P. Rohrmann, A. Hause, and F. Mitschke, Sci. Rep. **2**, 866 (2012); Phys. Rev. A **87**, 043834 (2013); A. Hause and F. Mitschke, *ibid.* **88**, 063843 (2013).

[23] R. Nath, P. Pedri, and L. Santos, Phys. Rev. A **76**, 013606 (2007).

[24] A. I. Yakimenko, V. M. Lashkin, and O. O. Prikhodko, Phys. Rev. E **73**, 066605 (2006); V. M. Lashkin, A. I. Yakimenko, and O. O. Prikhodko, Phys. Lett. A **366**, 422 (2007).

[25] B. P. Anderson and P. Meystre, Cont. Phys. **44**, 473 (2003).

[26] J. Cuevas, Boris A. Malomed, P. G. Kevrekidis, and D. J. Frantzeskakis, Phys. Rev. A **79**, 053608 (2009).

[27] F. Kh. Abdullaev and V. A. Brazhnyi, J. Phys. B: At. Mol. Opt. Phys. **45**, 085301 (2012).

[28] S. Sinha and L. Santos, Phys. Rev. Lett. **99**, 140406 (2007).

[29] C. Pare and P.-A. Belanger, Opt. Commun. **168**, 103 (1999); B.-F. Feng and B. A. Malomed, *ibid.* **229**, 173 (2004); S. M. Alamoudi, U. Al Khawaja, and B. B. Baizakov, Phys. Rev. A **89**, 053817 (2014).

[30] M. Abramowitz and I. A. Stegun, *Handbook of Mathematical Functions* (National Bureau of Standards, Washington, DC, 1964).

[31] S. Gholami, Ph. Rohrmann, A. Hause and F. Mitschke, Appl. Phys. B **116**, 43 (2014).

[32] J. A. Nelder and R. Mead, Comput. J. **7**, 308 (1965).

[33] R. Luus and T. H. I Jaakola, AIChE J. **19**, 760 (1973).

[34] S. M. Al-Marzoug and R. J. W. Hodgson, Opt. Commun. **265**, 234 (2006).

[35] H. S. Rag and J. Gea-Banacloche, Am. J. Phys. **83**, 305 (2015).